Proc. Natl. Acad. Sci. USA
Vol. 87, pp. 5643–5647, August 1990
Biophysics

Folding and activity of hybrid sequence, disulfide-stabilized peptides

(hybrid peptides/peptide folding/helix nucleation/immunogenic peptides)

JOSEPH H. B. PEASE, RICHARD W. STORRS, AND DAVID E. WEMMER*

Department of Chemistry, University of California, Berkeley, CA 94720

Communicated by Robert L. Baldwin, April 20, 1990

ABSTRACT **Peptides have been synthesized that have hybrid sequences, partially derived from the bee venom peptide apamin and partially from the S peptide of ribonuclease A. The hybrid peptides were demonstrated by NMR spectroscopy to fold, forming the same disulfides and basic three-dimensional structure as native apamin, containing a β-turn and an α-helix. These hybrids were active in complementing S protein, reactivating nuclease activity. In addition, the hybrid peptide was effective in inducing antibodies that cross-react with the RNase, without conjugation to a carrier protein. The stability of the folded structure of this peptide suggests that it should be possible to elicit antibodies that will react not only with a specific sequence, but also with a specific secondary structure. Hybrid sequence peptides also provide opportunities to study separately nucleation and propagation steps in formation of secondary structure. We show that in S peptide the α-helix does not end abruptly but rather terminates gradually over four or five residues. In general, these hybrid sequence peptides, which fold predictably because of disulfide bond formation, can provide opportunities for examining structure–function relationships for many biologically active sequences.**

It is well known that in disulfide cross-linked proteins the relative positions of cysteines are strongly conserved. Among families of proteins containing similar disulfides, there tends to be a strong conservation of the three-dimensional structure even when the overall sequence homology is rather low (1). Thus, it is clear that a wide variety of amino acid sequences can be accommodated within the fold defined by the cystine bridges. We have taken advantage of this adaptability to form structured, hybrid sequence peptides. In these hybrids the folding is largely controlled by formation of disulfides involving cysteines with relative positions taken from a natural peptide. However, many of the noncysteine residues can be replaced with a sequence from another protein. In the cases discussed here, the disulfides were derived from apamin (2–4), and the noncysteine amino acids from the helical region of apamin were replaced with those from the S peptide of RNase A (5). The S peptide, consisting of the first 20 amino acids from RNase A, has been extensively characterized and has been shown to have a helix-forming propensity (6–8) (existing as up to ≈40% helix under optimal conditions). In addition, there was shown to be a helix stop signal present (9, 10) near the 13th or 14th residue. This signal persists even in trifluoroethanol, where the overall helical fraction is significantly increased (11, 12). The S peptide binds (with an association constant of $\approx 10^6$) to S protein, the large fragment of RNase A from which it was cleaved, reactivating nuclease activity (3). In the apamin–S peptide hybrids, we show that the disulfides stabilize the helical segment at the beginning of the S peptide completely, giving us the opportunity to investigate the propagation of the helix after essentially perfect nucleation. Using two-dimensional NMR (13), we show that the first 16 residues of the hybrid fold into a structure essentially identical to that of the parent apamin and that the helix in the hybrid containing the full-length S peptide begins to be disrupted at the same position as in the isolated S peptide, although there is maintenance of some helical character for four or five residues. This indicates that the helix stop signal in this essentially isolated helix is not highly localized but rather is spread over several residues. We also show that the full hybrid peptide is immunogenic and elicits antibodies that cross-react with intact RNase A.

MATERIALS AND METHODS

The hybrid peptides were synthesized on an Applied Biosystems 430A synthesizer by *t*-butoxycarbonyl chemistry. HF cleavage was performed by Applied Biosystems, yielding 1.25 g of crude material (not all peptide). Then, 180 mg of the crude material was dissolved in 100 ml of 5 mM Tris·HCl (pH 8.0) and a molar excess of dithiothreitol. The peptide was allowed to air oxidize at room temperature for 1 week. The solution was reduced to 10 ml by lyophilization. HPLC was done on a Waters HPLC equipped with a Waters Delta Pak preparative column (C18 300 Å; 19 mm × 30 cm). A two-buffer system was used: buffer A, 0.1% trifluoroacetic acid/H_2O; buffer B, 0.1% trifluoroacetic acid/60% CH_3CN/40% H_2O. The run started, at a flow rate of 4 ml/min, with 100% buffer A for 5 min, then a linear gradient to 30% buffer B over 10 min, and finally a linear gradient to 70% buffer B over 80 min. The hybrid II peptide eluted at 58% buffer B and was the major peak at 235 nm. Approximately 60 mg of purified peptide was obtained from the 180 mg of crude starting material. Hybrid I was synthesized and purified in the same way, but the overall yield was significantly lower. The correct identity of the peptides was confirmed by FAB mass spectroscopy as well as by NMR spectroscopy.

NMR measurements were carried out on a GN-500 spectrometer. Samples were dissolved in 100 mM NaCl (pH 2.5), and two-dimensional spectra were run at 20°C. For the nuclear Overhauser effect spectrum (NOESY) shown, a mixing time of 450 ms was used. The hybrid I sample was ≈5 mM, while hybrid II was ≈10 mM.

CD measurements were carried out on a Jasco J500 spectropolarimeter. Samples were at ≈10 μM concentration in the same buffer used for NMR, at ambient temperature, in 0.2-cm cells.

Studies of complementation of RNase S by the peptides were carried out by mixing 2 μl of either authentic S peptide (200 or 2 μM; Sigma), a hybrid (200 or 2 μM), or water (control) with 2 μl of S protein (3.6 μM; Sigma). These were mixed and allowed to stand at room temperature for 10 min to allow association of the peptide. Ten microliters of RNA (18 S + 23

The publication costs of this article were defrayed in part by page charge payment. This article must therefore be hereby marked "*advertisement*" in accordance with 18 U.S.C. §1734 solely to indicate this fact.

Abbreviation: NOE (SY), nuclear Overhauser effect (spectroscopy).
*To whom reprint requests should be addressed.

```
          1   3   5   7   9  11  13  15  17  19  21  23  25
          |   |   |   |   |   |   |   |   |   |   |   |   |
S-peptide             K E T A A A K F E R Q H M D S S T S A A
apamin    C N C K A P E T A L C A R R C Q Q H
hybrid-I  C N C K A P E T A A C K F E C Q H M
hybrid-II C N C K A P E T A A C K F E C Q H M D S S T S A A
```

FIG. 1. The sequences of S peptide, apamin, and the two hybrids used in this work are given (using standard one-letter codes), with the residue numbering indicated.

S; Boehringer Mannheim) at 80 μg/ml in 0.1 M NaOAc (pH 5) at 0°C was added and quickly mixed. After a reaction time of 15–60 s the reaction was quenched by the addition of 50 μl of phenol/chloroform (1:1) and mixing. The water layer was then separated, RNA was precipitated with cold ethanol, resuspended in 30% (vol/vol) glycerol, run on 1.2% agarose gels, and visualized with ethidium bromide. Initial separate bands for the 18S and 23S RNA components disappeared and were replaced by broad bands of cleavage products running faster on the gel. Controls were also run with hybrid peptide alone, S peptide alone, and S protein alone. No cleavage was seen for the peptides; however, a slow cleavage (relative to RNase A or the peptide complexes) was seen with S protein alone (probably resulting from contamination with RNase S).

Hybrid II (sequence given in Fig. 1) was also used to induce antibodies in rabbits. Following standard methods, three rabbits were immunized with the unconjugated peptide in

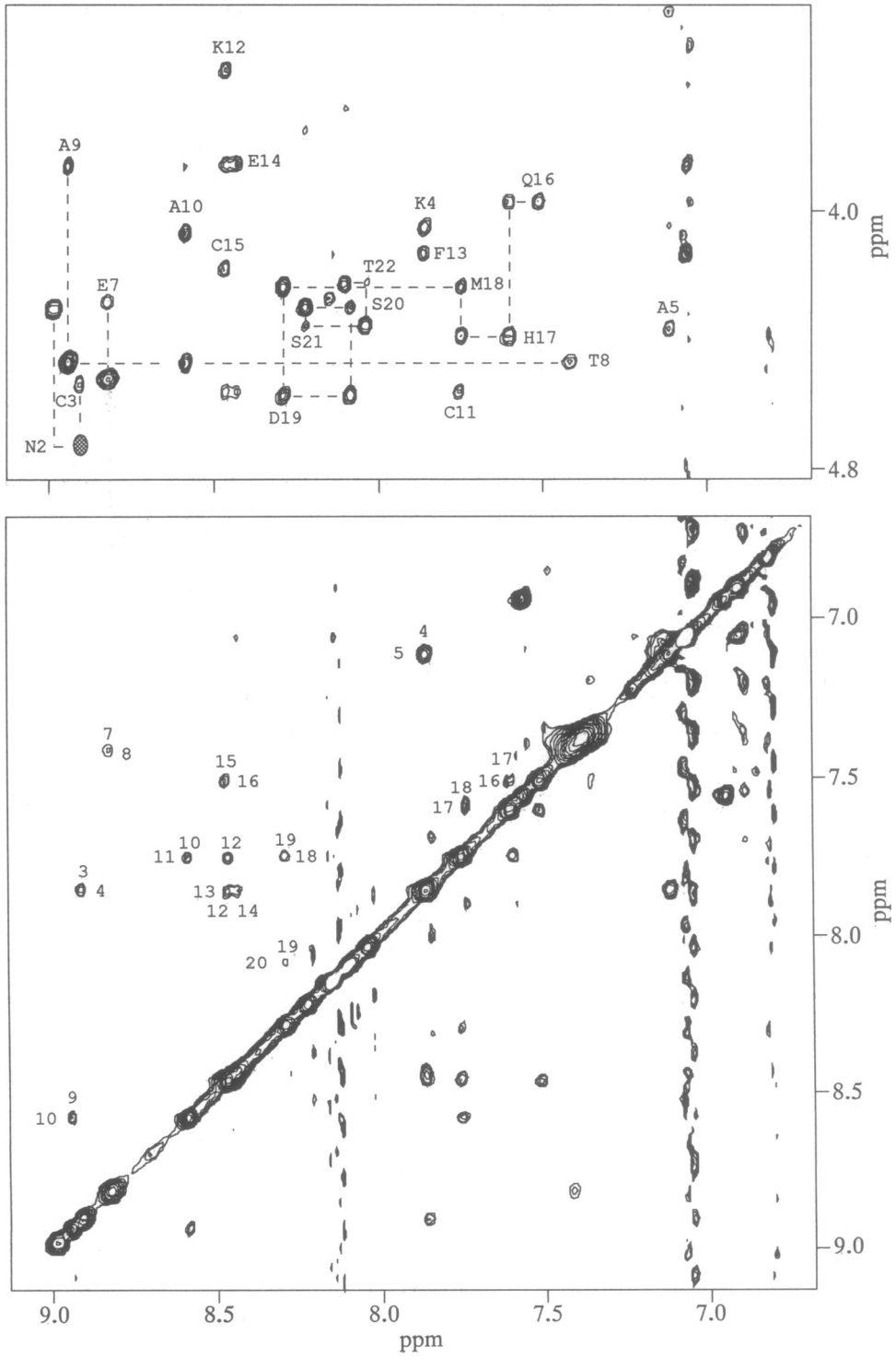

FIG. 2. Amide to α proton (*Upper*) and amide to amide (*Lower*) cross-peak regions of a NOESY spectrum of hybrid II in H_2O solution. In the upper region, peaks are labeled at the position of the intraresidue amide to α position. Dashed lines indicate amide to preceding α connectivities. In this spectrum, the α proton of residue 2 was under the solvent peak and was saturated. The position of the cross-peak from C-3 to N-2 seen at lower temperature is indicated by a shaded oval. In the lower region, cross-peaks are labeled with the two residues from which they arise.

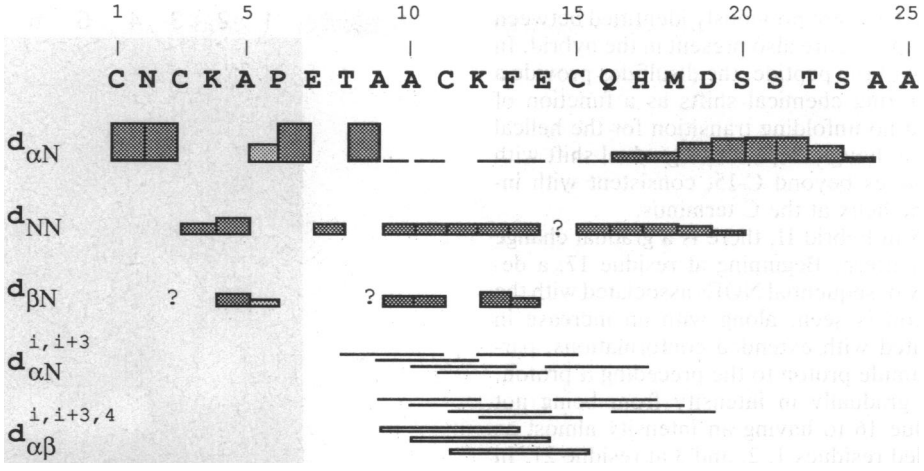

FIG. 3. Summary of sequential connectivities seen for hybrid II. The shaded bars for $d_{\alpha N}$, d_{NN}, and $d_{\beta N}$ indicate observed connectivities, and the height of the bar indicates the intensity of the observed cross-peak. Question marks indicate cross-peak positions that are either obscured by other peaks or are too near the diagonal to be seen. For some peaks, the data in Fig. 2 were supplemented by a second NOESY run at 5°C, in which some peaks shifted sufficiently to remove degeneracies. The i, $i+3$ connectivities are indicated by lines that do not represent intensities. The i, $i+4$ cross-peaks are indicated by double bars.

Freund's adjuvant at 1-month intervals. To assay the activity of antibodies in the serum, microtiter wells were coated with RNase and then treated with bovine serum albumin to block remaining sites. Controls were treated with bovine serum albumin alone. Dilutions of serum were done with buffered saline containing Triton X-100 and bovine serum albumin. Although the background is high at low dilution, there is clear reactivity to RNase A.

RESULTS

The sequences of apamin, S peptide, and the two hybrids of apamin and the S peptide are shown in Fig. 1. The numbering of residues used is based on the apamin sequence. The first, hybrid I, consists of only the residues of the S peptide which are in a helical conformation in RNase and, correspondingly, are partially helical in the free peptide in solution as well. The second, hybrid II, has the full length S peptide incorporated. When the peptides are air oxidized in dilute solutions, they fold spontaneously to the apamin-like structure [conditions under which synthetic apamin also folds into its active structure (14–16)]. CD spectra of apamin and the two hybrid peptides are essentially identical in shape (data not shown), with a maximum negative ellipticity near 208 nm and a distinct shoulder arising from the helix at 220 nm (17), providing evidence that the peptides fold similarly.

The solution structures of the peptides were characterized by two-dimensional NMR and distance geometry methods (18–20), as had been applied to apamin (21, 22) and many other proteins (13). Relevant sections of the two-dimensional NOESY spectrum are shown in Fig. 2, and a summary of the sequential connectivities is shown in Fig. 3 for hybrid II. The pattern of sequential connectivities for residues 1–18 of both hybrids is identical to that observed for apamin, indicating that the overall folding is very similar. In moderate salt conditions, such as those used here, there is no evidence for aggregation of either S peptide or apamin. Although extensive tests were not carried out on the hybrids, we have found no evidence for their aggregation.

Peak intensities from NOESY spectra of hybrid II were used to derive interproton distance constraints. These were used with the distance geometry program DSPACE (Hare Research) to derive structures that are consistent with the observed data for residues 1–18. As discussed below, the residues beyond 18 are dynamically disordered, and it is not meaningful to try to derive a structure with this method. The results of these calculations are shown in Fig. 4, a superposition of five of the resulting structures, which have an rms variation in backbone atom positions of ≈0.5 Å for the first 16 residues. A detailed comparison of these structures with those calculated for apamin shows that there are only very minor differences. Superposition of the backbone atoms of apamin with those of the hybrid results in rms fits of ≈1.0 Å. This similarity is not surprising, since there are relatively few amino acid differences, and they all occur in the helical

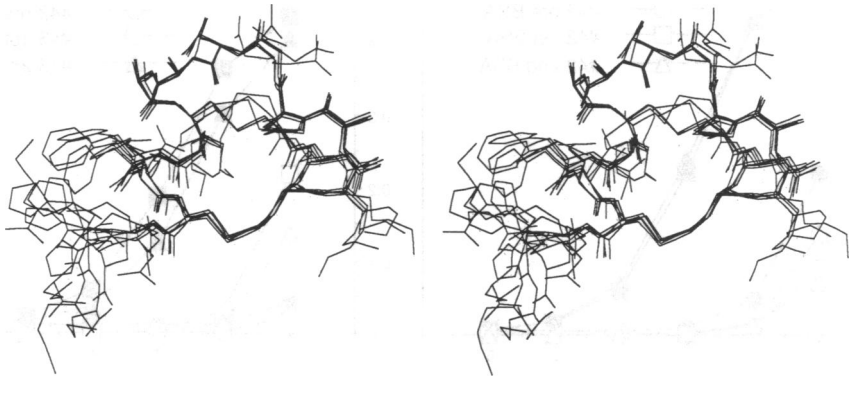

FIG. 4. A stereo drawing of five distance geometry derived structures of residues 1–18 of hybrid II, including all non-hydrogen atoms. Structures were superimposed by minimizing rms deviations for backbone atom positions of residues 1–16. The calculations were carried out as described in ref. 13. The helical segment, containing residues 9–16, is clearly visible at the left. The helix becomes disordered beyond this point, as discussed in the text.

region. The contacts that were previously identified between the turn and helix in apamin are also present in the hybrid. In spite of the small size of the peptide, the disulfides provide a high stability. Monitoring chemical shifts as a function of temperature revealed no unfolding transition for the helical residues up to 80°C, although there was a gradual shift with temperature for residues beyond C-15, consistent with increased fraying of the helix at the C terminus.

Beyond residue 18 in hybrid II, there is a gradual change in the connectivity pattern. Beginning at residue 17, a decrease in the intensity of sequential NOEs associated with the α-helical conformation is seen, along with an increase in those NOEs associated with extended conformations, particularly from each amide proton to the preceding α proton. The latter increase gradually in intensity from being not observable for residue 16 to having an intensity almost as large as fully extended residues 1, 2, and 3 at residue 21. In addition, the long-range (i, i+3; and i, i+4) helical NOEs (23) are also lost beyond residue 18. This pattern suggests strongly that the helix becomes dynamically disordered (24, 25), beginning at residue 17, with the fraction of time spent in the helical conformation decreasing gradually from residue 17–21. This interpretation is further strengthened by the observation that all NOEs for residues 23–25 are greatly reduced in intensity, including those corresponding to fixed distances, such as the α proton to methyl on alanines 24 and 25. Since the other alanine residues have strong NOE cross-peaks between these protons, as expected, the reduced intensity must come from a change in the effective correlation time for the motion of the internuclear vectors. The bulk of the peptide rotates sufficiently slowly that negative NOEs are seen in spite of the relatively low molecular weight. Just a moderately small decrease in correlation time could make these protons reach the zero crossing in NOE intensity. This observation is qualitatively similar to that of Rico *et al.* (26), who found a change in the sign of the NOE in this region of the isolated S peptide and also interpreted it as increased mobility of this segment. Our data are consistent with the C-terminal eight residues of the peptide being dynamically disordered, with a gradually decreasing correlation time for internal motion toward the C terminus of the peptide.

These data show that the helix stop signal identified in this region is not abrupt but rather represents a progressively lower fraction of time spent in helical conformations for successive residues over a stretch of five residues, ≈1.5 helical turns. This pattern is qualitatively similar to what one would predict from the helix propagation values, s, derived from host–guest data, assuming that the helix is perfectly nucleated at residue 15. With values from the literature (1), the fraction helix that is predicted for each residue (assuming 100% helix at residue 15 and simply multiplying by the successive s values) is

15					20					25
C	Q	H	M	D	S	S	T	S	A	A
(1.00)	0.96	0.77	0.90	0.59	0.46	0.35	0.30	0.22	0.24	0.25

These values correlate fairly well with the observed NOE pattern, out to about residue 20. Beyond this, it is difficult to assess because of increased mobility, but probably the percentage helix drops more quickly than predicted. It is clear

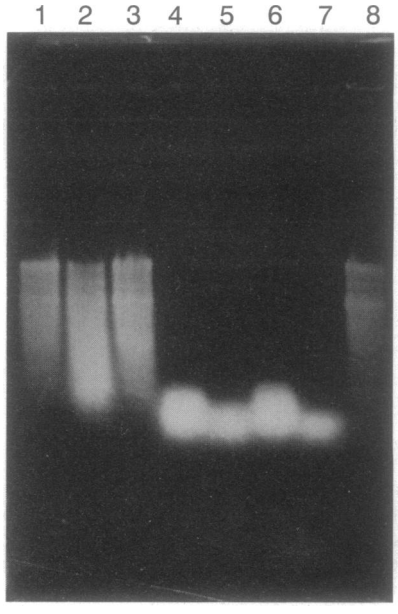

FIG. 5. Ethidium-stained agarose gel showing hydrolysis of a mixture of 18S and 23S RNA by reconstituted RNase, as described. Lanes: 1, RNA only; 2, S protein only, 15-s reaction; 3, S protein only, 60-s reaction; 4, S protein + hybrid II, 15-s reaction; 5, S protein + hybrid II, 60-s reaction; 6, S protein + S peptide, 15-s reaction; 7, S protein + S peptide, 60-s reaction; 8, hybrid II only, 60-s reaction.

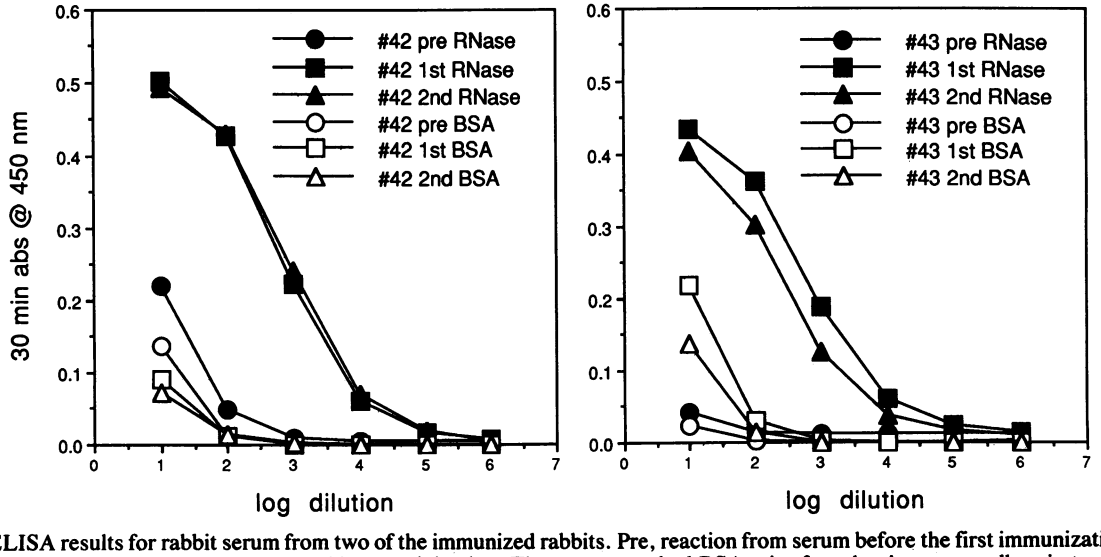

FIG. 6. ELISA results for rabbit serum from two of the immunized rabbits. Pre, reaction from serum before the first immunization; 1st, after the first booster injection; 2nd, after the second booster injection. The curves marked BSA arise from bovine serum albumin treatment of the wells rather than RNase A.

that the largest residue-to-residue difference in the NOEs is from M-18 to D-19, which is predicted by the helix propagation parameters. This behavior might be somewhat different for free S peptide, since in general both nucleation and propagation will affect the fraction of helix at any particular residue, and the nucleation parameter, σ, is strongly dependent on amino acid.

Using the distance geometry structure of hybrid II, we carried out modeling of the complex of hybrid II with S protein. The exposed face of the helix in this hybrid corresponds to the buried face of the S peptide when it is bound in RNase. The extra residues, corresponding to the β-turn and loop of apamin, protrude out from the surface of the enzyme. We carried out complementation studies of RNase S with both hybrids by examining the cleavage of a mixture of 18S and 23S RNA, examined on agarose gels. We find that both peptides restored activity to a level essentially equivalent to that found with the S peptide itself either with peptide in excess or with near stoichiometric mixtures (Fig. 5). Hybrid sequence peptides of RNase with angiogenin, which confer modified activity with RNAs, have also been made (27). In this case, the intent was to transfer substrate specificity rather than to stabilize a particular secondary structure, as in our case.

In two of the rabbits immunized with hybrid II, antibodies were produced that cross-react with native RNase A by ELISA (Fig. 6). Although these are polyclonal antibodies, the fairly good cross-reaction of the anti-peptide antibodies with native RNase is of interest. It suggests (although it does not prove conclusively) that the antibodies recognize the helical conformation of the hybrid peptide.

DISCUSSION

These studies demonstrate clearly that the use of disulfides to stabilize a particular peptide fold does not interfere with activity, provided that the contact face is appropriately exposed and that the stabilized secondary structure is the correct one. In the example discussed here, a helical conformation was required for activity. Hybrid peptides of this general construction should thus be useful for testing hypotheses about the active conformations of peptides. Similar approaches using nonpeptide covalent constraints have already been used in the design of various drugs, hormones, and other small biologically active molecules. The use of disulfides to this end is convenient because of the ease of peptide synthesis. By studying natural disulfide stabilized peptides, it should be possible to map a sequence of interest on a variety of different secondary structures. These hybrid peptides also provide excellent models for understanding certain aspects of protein folding, such as propagation of nucleated helices as discussed above. Since the helical segments of the peptides are very stable, these hybrids should provide a mechanism for targeting antibodies both to a particular sequence and also to a helical conformation by transferring a protein segment into this hybrid framework.

We would like to thank Mr. David Koh for help with peptide synthesis, Ann Caviani Pease for help with the RNase activity assays, Prof. I. Tinoco, Jr., for access to his CD instrument, Prof. Peter Kim for producing the antibodies and for helpful discussions, and the National Science Foundation for financial support through Grant DMB 8815998. We would also like to acknowledge equipment grants from the Department of Energy (DE F605 86ER75281) and National Science Foundation (DMB 8609035).

1. Creighton, T. E. (1984) *Proteins, Structures and Molecular Properties* (Freeman, New York), pp. 252–264.
2. Habermann, E. & Reiz, K. G. (1965) *Biochem. Z.* **343,** 192–203.
3. Callewaert, G. L., Shipolini, R. & Vernon, C. A. (1968) *FEBS Lett.* **1,** 111–113.
4. Shipolini, R., Bradbury, A. F., Callewaert, G. L. & Vernon, C. A. (1967) *Chem. Commun.* **14,** 679–680.
5. Richards, F. M. & Vithayathil, P. J. (1959) *J. Biol. Chem.* **234,** 1459–1465.
6. Brown, J. E. & Klee, W. A. (1971) *Biochemistry* **10,** 470–476.
7. Bierzynski, A., Kim, P. S. & Baldwin, R. L. (1982) *Proc. Natl. Acad. Sci. USA* **79,** 2470–2474.
8. Kim, P. S., Bierzynski, A. & Baldwin, R. L. (1982) *J. Mol. Biol.* **162,** 187–199.
9. Rico, M., Neito, J. L., Santoro, J., Bermejo, F. J., Herranz, J. & Gallego, E. (1983) *FEBS Lett.* **162,** 314–319.
10. Kim, P. S. & Baldwin, R. L. (1984) *Nature (London)* **307,** 329–334.
11. Nelson, J. W. & Kallenbach, N. R. (1986) *Proteins* **1,** 211–217.
12. Nelson, J. W. & Kallenbach, N. R. (1989) *Biochemistry* **28,** 5256–5261.
13. Wüthrich, K. (1986) *NMR of Proteins and Nucleic Acids* (Wiley, New York), pp. 117–202.
14. Granier, C., Pedroso Muller, E. & van Reitschoten, J. (1978) *Eur. J. Biochem.* **82,** 293–299.
15. Cosand, W. L. & Merrifield, R. B. (1977) *Proc. Natl. Acad. Sci. USA* **74,** 2771–2775.
16. van Reitschoten, J., Granier, C., Rochat, H., Lissitzky, S. & Miranda, F. (1975) *Eur. J. Biochem.* **56,** 35–40.
17. Hider, R. C. & Ragnarsson, U. (1981) *Biochim. Biophys. Acta* **667,** 197–208.
18. Havel, T., Kuntz, I. D. & Crippen, G. M. (1983) *Bull. Math. Biol.* **45,** 665–720.
19. Havel, T. & Wüthrich, K. (1984) *Bull. Math. Biol.* **46,** 673–698.
20. Wagner, G., Braun, W., Havel, T. F., Schaumann, T., Go, N. & Wüthrich, K. (1987) *J. Mol. Biol.* **196,** 611–639.
21. Wemmer, D. & Kallenbach, N. R. (1983) *Biochemistry* **22,** 1901–1906.
22. Pease, J. H. B. & Wemmer, D. E. (1988) *Biochemistry* **27,** 8491–8499.
23. Wüthrich, K., Billeter, M. & Braun, W. (1984) *J. Mol. Biol.* **180,** 715–740.
24. Dyson, H. J., Rance, M., Houghten, R. A., Lerner, R. A. & Wright, P. E. (1988) *J. Mol. Biol.* **201,** 161–200.
25. Dyson, H. J., Rance, M., Houghten, R. A., Lerner, R. A. & Wright, P. E. (1988) *J. Mol. Biol.* **201,** 201–217.
26. Nieto, J. L., Jimenez, M. A., Rico, M., Santoro, J. & Herranz, J. (1988) *FEBS Lett.* **239,** 83–87.
27. Harper, J. W., Auld, D. S., Riordan, J. F. & Vallee, B. L. (1988) *Biochemistry* **27,** 219–226.